Model of radial basis functions with slope-based shape factor and distribution for optical freeform surface

Liuchang Xiao,[a] Kainian Tong,[a] Lipei Song,[a] Lingjie Wang,[b] Pengfei Wu,[a,c] Weiwei Liu,[a,d] and Xing Zhao[a,d,*]

[a]Nankai University, Institute of Modern Optics, Tianjin, China

[b]Chinese Academy of Sciences, Changchun Institute of Optics, Fine Mechanics and Physics, Key Laboratory of Optical System Advanced Manufacturing Technology, Changchun, China

[c]Tianjin Key Laboratory of Optoelectronic Sensor and Sensing Network Technology, Tianjin, China

[d]Tianjin Key Laboratory of Micro-scale Optical Information Science and Technology, Tianjin, China

Abstract. To obtain satisfactory performance in characterizing optical freeform surfaces with local features, this paper proposes a model of a radial basis function with slope-based shape factor and distribution (RBF-SSD). Compared to previous RBF-slope models with only slope-based shape factors, the RBF-SSD model relates both shape factors and distribution with the surface slope, ensuring greater fitting ability can be achieved when fitting a surface with local features. Fitting experiments for two different surfaces demonstrated the fitting ability of the RBF-SSD model. An off-axis three-mirror system with $3° \times 3.6°$ field of view was designed as an example to show the optical design efficacy of our model. © *2020 Society of Photo-Optical Instrumentation Engineers (SPIE)* [DOI: 10.1117/1.OE.59.12.125101]

Keywords: optical freeform surface; radial basis function; design.

Paper 20200729 received Jun. 19, 2020; accepted for publication Nov. 18, 2020; published online Dec. 3, 2020.

1 Introduction

With more degrees of design freedom, optical freeform surfaces are playing important roles in the design of optical systems, especially off-axis optical systems. Owing to their arbitrary shapes, freeform surfaces can provide enhanced aberration control and high optical performance, thus leading to a smaller number of elements and lighter system weight.[1–5] The emergence of single-point diamond turning enables the fabrication of non-rotationally symmetric free-form surfaces. In the design of optical systems with optical freeform surfaces, it is necessary to find a proper mathematical model to characterize the freeform surface because different models will exhibit different fitting features. The Zernike polynomial model,[6] which contains a polynomial sequence orthogonal to the unit circular disk and is closely related to the Seidel aberration, is a popular optical freeform surface model. This model has been widely used in the fields of surface characterization, optical design, and optical testing.[7,8] Another practical freeform surface model is the Q-type polynomial, which offers a rough interpretation of the shape at a glance and facilitates a range of estimates of manufacturability.[9,10] Both the Zernike polynomial and Q-type are global models, which means any changes of the coefficient of any term in the polynomial will influence the sag value of the whole aperture when fitting a surface. This leads to deterioration of fitting performance for complicated or asymmetric surfaces, and thus additional polynomial terms or special sample grid distributions are needed for a satisfactory performance.[11,12] To obtain better performance in the design of freeform surfaces, the radial basis function (RBF) model was first introduced in optical design by Cakmakci et al.[13,14] The surface described by the RBF model is formed by a certain number of independent RBFs in which each basis has limited influence on the entire aperture scope. Therefore, the RBF model is a local-type freeform surface model and

*Address all correspondence to Xing Zhao, zhaoxingtjnk@nankai.edu.cn

0091-3286/2020/$28.00 © 2020 SPIE

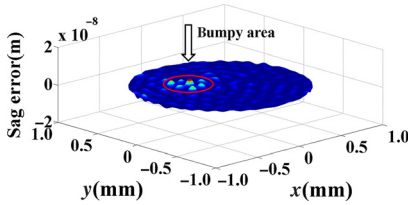

Fig. 1 Fitting error in 0.8-aperture as fitted by RBF-Slope model with 784 basis functions.

has great potential to be used to balance large aberrations in asymmetric systems, which always have strong local variations.

Although the original RBF model proposed by Cakmakci et al.[15] has some successful applications in optical system design,[16,17] its fitting ability is still limited for inefficient distribution and identical shape factors. To improve the fitting ability of the RBF model, some new RBF models have been proposed. Anisotropic RBF models with adaptive grid refinement have been introduced in Ref. 18, which refine the local RBF distribution until the global error is below the specified value and shows an improved fitting ability when fitting complicated surfaces. However, the adaptive grid refinement method is computationally expensive and time-consuming because of the self-adaptive process. We recently proposed a new RBF-slope model, which establishes the relationship between the shape factor and surface slope without the need for complex and repeated computations,[19] and then fabricated the single mirror magnifier represented by the RBF-slope model using single-point diamond turning method.[20] However, it should be recognized that most basis functions of this model are still nearly uniformly distributed over the aperture, which also limits the model's fitting ability for large local surface shape variations. As can be seen in Fig. 1, when fitting a paraboloid with a bump, even for a 784 basis (a very large number), the fitting error in the bumpy area is clearly larger than the error of other areas. Thus, the RBF-slope model is not appropriate for characterizing surfaces with large slope variations if high fitting precision is expected. To achieve high fitting precision for local-feature surfaces, we propose the RBF with slope-based shape factor and distribution (RBF-SSD) model in this paper, which relates both shape factor and distribution with surface slope.

The remainder of this paper is organized as follows: Sec. 2 briefly introduces the RBF-Slope model and RBF-SSD model, and compares the fitting features of these two models in principle. Then, the fitting experiments for a double-curved freeform surface and a bumpy paraboloid with two RBF models is presented to demonstrate the better fitting ability of the RBF-SSD model in Secs. 3 and 4, respectively. In Sec. 5, we show the design process of an off-axis three-mirror system with the RBF-SSD model and the optical performances of different freeform surface models are compared and analyzed.

2 RBF-SSD Model

2.1 *RBF-Slope Model*

In general, the sag of a freeform surface can be represented by a base conical shape and an additional sum of basis functions. For the RBF model, the mathematical form can be expressed as follows:

$$\begin{aligned} z(x,y) &= \frac{c(x^2+y^2)}{1+\sqrt{1-(1+k)c^2(x^2+y^2)}} + \sum_i w_i \varphi_i(\|\vec{r}-\vec{r}_i\|) \\ &= \frac{c(x^2+y^2)}{1+\sqrt{1-(1+k)c^2(x^2+y^2)}} + \sum_i w_i e^{-\varepsilon_i^2((x-x_{0i})^2+(y-y_{0i})^2),} \end{aligned} \tag{1}$$

where $z(x,y)$ denotes the sag of the freeform surface in the aperture, c is the vertex curvature, and (x,y) are the Cartesian coordinates. The second term represents the combination of RBF $\phi_i(\|\vec{r}-\vec{r}_i\|)$, where $\vec{r}$ denotes a vector pointing to any location in the aperture, $\vec{r}_i$ is the vector pointing to the center of the RBF, and $\|\cdot\|$ is the Euclidean norm with w_i denoting the

coefficients. The function can typically take the Gaussian form, as indicated in the second form of the equation. The use of the Gaussian function offers the following advantages: smoothness, approximate local characteristics (the value of Gaussian function rapidly reduces with the increase in the distance away from the center), and good analyticity of solution.[14] The parameter (x_{0i}, y_{0i}) and shape factor ε_i determine the center position and the width of the basis function, respectively. According to local properties of Gaussians, the shape factor ε_i of each basis function determines its influence range; a larger shape factor induces a smaller range and sharper basis function. This local property of the basis function sequence distribution throughout the aperture enables higher fitting ability in the Gaussian RBF than the Zernike polynomial, which leads to greater advantages of the RBF model for characterizing asymmetrical optical freeform surfaces.

As a new RBF model, the RBF-Slope model builds the relationship between the shape factor and surface slope, leading to improved characterization ability compared with conventional RBF models.[19] The RBF-slope model follows two principles. The first is that all the centers of the basis function sequence are distributed within the aperture to avoid the waste of basis outside of the aperture. The second principle is that the shape factor ε_i of each basis function is set to be proportional to the peak-to-valley value of the surface sag in corresponding unit, which can be described by the following equation:

$$\varepsilon_i = k\frac{PV_i}{S_i}, \tag{2}$$

where PV_i denotes the peak-to-valley value of the surface sag in unit i and S_i is the area of this unit. Coefficient k is related to the average shape factor specified in advance. According to this principle, the relationship between the shape factor and surface slope has been built. The shape factor can vary with the responding surface slope across the surface, allowing the basis functions to be either flatter or more peaked depending on what is needed, adding to the flexibility of the RBF model. This allows the RBF-slope model to be appropriate to fit surfaces with different slopes such as asymmetric surfaces.

2.2 *RBF-SSD Model*

Although the RBF-slope model relates the shape factor and surface slope and works better in surface fitting than the original RBF model, a serious problem resulting from uniform distribution still exists that limits the model's fitting ability. As shown in Fig. 2, when fitting a surface region with large slope (sharp area), the shape factors within this region will be set to be large. If the density of basis functions is large enough, then there will be a serious gap between neighboring basis in the sharp region leading to a poor fit. Therefore, the characterizing ability of the model will be limited. To solve this problem and to further improve the fitting ability of the RBF model, we propose an RBF-SSD model in this paper.

Based on the RBF-slope model, the RBF-SSD model also follows the two principles of RBF-slope, i.e., all the centers of the basis function sequence are distributed within the aperture, and

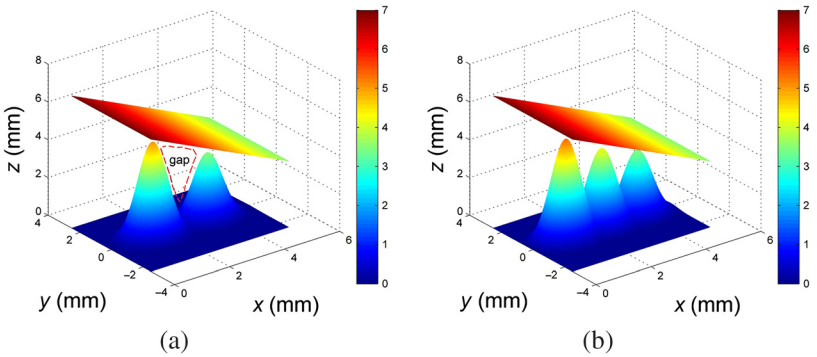

Fig. 2 Basis functions for RBF-Slope model (a) and RBF-SSD model (b) when fitting a sharp surface region.

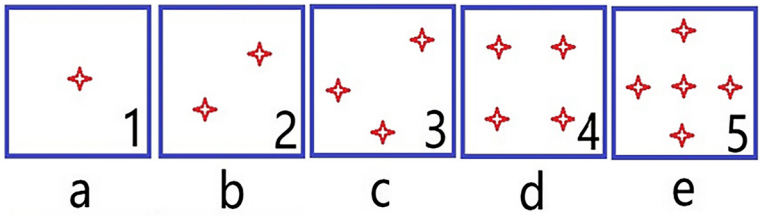

Fig. 3 The distribution for different basis number.

the shape factor is proportional to the surface slope. In addition, to avoid the decrease of the fitting accuracy of the model at the edge of the aperture, a certain number of basis functions are deliberately set at the edge of the aperture. Apart from these two principles, to improve the distribution of basis, the basis density of the RBF-SSD model is also set to be nearly proportional to the surface slope; this is the third principle of this model. As shown in Fig. 2, according to the third principle, under the situation of a fitting surface region with a large slope, there will be more basis for fitting. Comparing Figs. 2(a) and 2(b), we can see the gap between the two basis sets can be eliminated by adding more basis, which means increasing the basis density in this region. With a slope-based shape factor, adding slope-based basis distribution in the meantime, the RBF-SSD model has more potential to obtain a better surface fitting performance.

The rule for determining the basis distribution when fitting a surface with a circular aperture can be described in the following steps. First, divide the aperture into $n \times n$ square units, where n is close to the root of basis number N. Then, determine the basis number in each unit according to the surface slope of the unit. It is impossible to make basis numbers in every unit be accurately proportional to the surface slope when the total basis number is not large enough; thus, there will be some units with the same basis number when their surface slopes are close. The relationship between basis number d_i and surface slope S_i in unit i can be described by following equation:

$$d_i = \text{floor}\{N * [S_i/\text{sum}(S_i)]\}, \tag{3}$$

where floor means rounding down the following number. After determining the basis number of each unit, the distribution for different basis number in every unit is shown in Fig. 3.

The distributions for basis numbers of 1, 2, 3, and 4 are shown in Figs. 2(a)–2(d), respectively. These distribution patterns are chosen to make the distribution as uniform as possible when there are many contiguous units with the same basis number. If the basis number equals or exceeds five, then one basis is located on the center of unit and other basis are uniformly distributed on a circle around the unit center.

The last step of this process is making the basis outside the aperture uniformly arranged around the edge of the aperture to ensure that every basis function affects the sag of the target surface. Next, we performed two fitting experiments with the RBF-slope model and RBF-SSD model, to explore the fitting performance of the proposed new model.

3 Fitting for Paraboloid with Bump

To demonstrate the fitting ability of the RBF-SSD model, we chose a paraboloid with a bump as the target surface for fitting. The sag of surface can be described with following equation:

$$z = \frac{(x^2+y^2)}{80} + 0.050e^{-0.25[(x-7)^2+(y+6)^2]} + 0.6e^{-0.49[(x+3)^2+(y-2)^2]} + 0.03e^{-0.81[(x-5)^2+(y-7)^2]}. \tag{4}$$

The surface was formed by a paraboloid and three Gaussian functions. The three Gaussian functions formed an obvious local variation in the paraboloid surface, as shown in Fig. 4. Fitting this bumpy surface with local variation, the features of different RBF models would be obvious. Therefore, the RBF-slope model and RBF-SSD model are applied to fit this surface to compare their fitting performance.

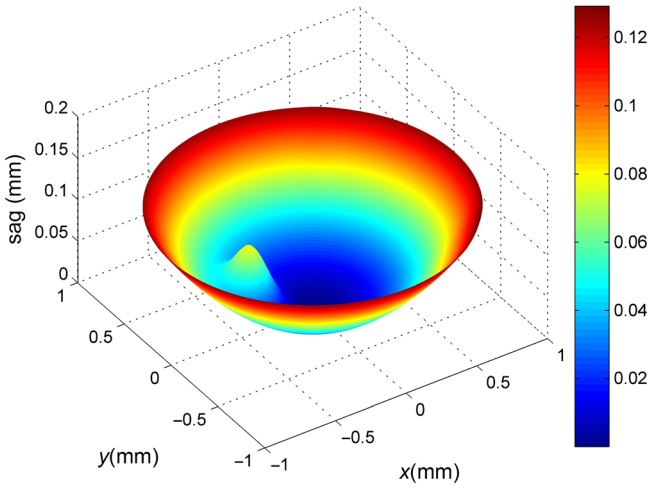

Fig. 4 Sag of paraboloid with a bump.

The basis numbers of both models are 484, which is large enough to obtain a sub-nm order fitting precision in this fitting. Around 6000 sample points are chosen to create the database, which are uniformly and regularly distributed in the entire aperture. The average shape factors of the two RBF models vary from 2 to 7, such that the best shape factor values of both models are within this range after some pre-experiments. The fitting problems are solved by the least-squares method. To deal with the ill-condition problems of least squares, the Householder transformation was used in the fitting process.[21]

Figure 5 shows the fitting results of the RBF-slope model and RBF-SSD model, where the fitting precision was evaluated by the logarithm of root mean square (RMS) errors for different average shape factors. Both RBF models showed low RMS, which denotes high fitting precision, in the shape factor range of 2 to 7. The RBF-SSD model even exhibited ∼1 order higher precision than the RBF-Slope model in the range of 3 to 6. With other shape factors out of the range of 2 to 7, the RBF-SSD model did not show obviously better fitting performance, because these average shape factor values did not match the basis number and distribution of model. However, only the best shape factor is of great interest.

Figures 6(a) and 6(b) show the shape factors over the entire aperture for two RBF models with the average shape factor of 5, which is the best average shape factor of the RBF-SSD model. For the RBF-Slope model, only shape factors were related to surface slope. However, for the RBF-SSD model, apart from shape factors, the basis distribution was also related to surface slope, which can be seen from the observation that the basis in the edge and the bump is denser than other area. The fitting RMS of two RBF models with average shape factor of 5 are shown in Figs. 6(c) and 6(d) for comparison. It can be clearly seen that the fitting error of the RBF-Slope

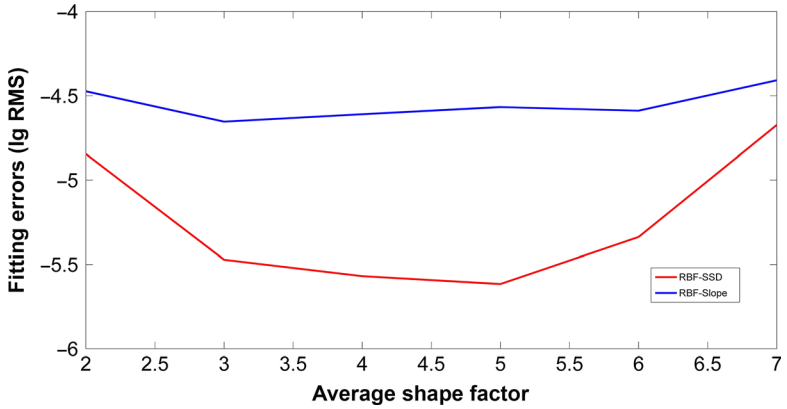

Fig. 5 Fitting performances of RBF-Slope and RBF-SSD models

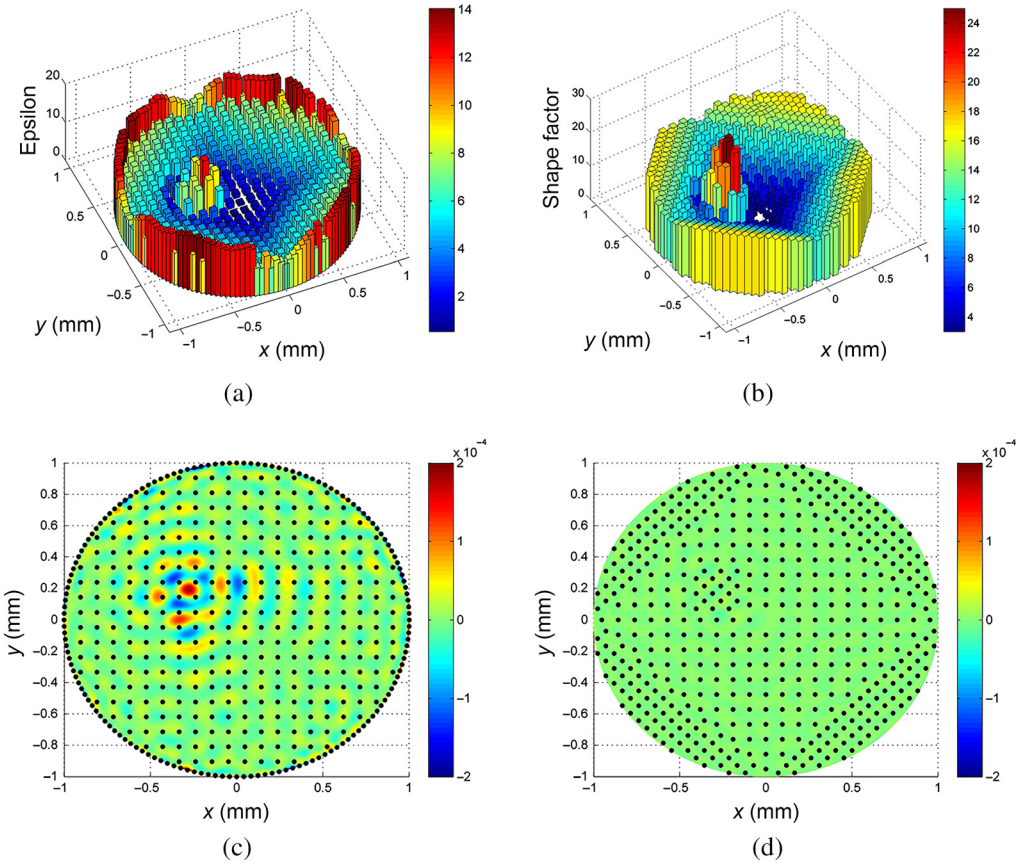

Fig. 6 Shape factors of (a) RBF-slope model and (b) RBF-SSD model. Fitting errors for (c) RBF-slope model and (d) RBF-SSD model.

Table 1 Results of fitting the paraboloid with a bump using different models.

Models	RMS (mm)	PV (mm)
RBF-direct	2.6144×10^{-5}	7.4876×10^{-4}
RBF-slope	2.7094×10^{-5}	4.8810×10^{-4}
RBF-SSD	2.4215×10^{-6}	4.6838×10^{-5}

model in the bumpy region was more serious than those of other regions, because the basis number in this region is not enough to match large shape factors or sharp basis. For the RBF-SSD model, the denser basis distribution in regions with large slope variation corresponds to larger sharper shape factors to achieve a better fitting result, which is demonstrated in Fig. 6(d). We can see that the fitting error remained small without an obvious change over the whole aperture, indicating that the RBF-SSD model showed better fitting performance than the RBF-Slope model for this bumpy surface. Table 1 compares the fitting accuracy of different models to this surface numerically, which also proves that RBF-SSD has the strongest fitting ability.

4 Fitting for a Double-Curved Freeform Surface

The fitting experiment for a bumpy paraboloid demonstrated the improved fitting ability of the RBF-SSD model. However, an optical surface rarely has a bump. To investigate the fitting performance of the model for a real optical surface, we used the RBF-SSD model in the fitting for

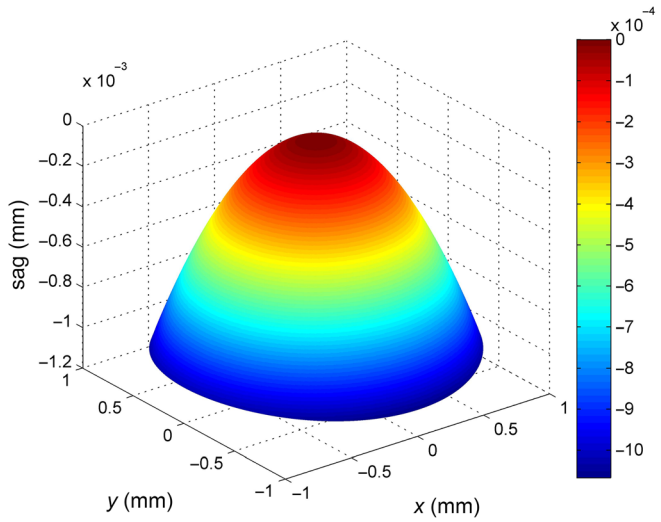

Fig. 7 Sag of double-curved freeform surface.

a double-curved freeform surface, which is a smooth optical surface, as plotted in Fig. 7. The expression of this surface is

$$z = \frac{(c_x x^2 + c_y y^2)}{1 + \sqrt{1 - ((1 + k_x)c_x^2 x^2 + ((1 + k_y)c_y^2 y^2)}} + \sum_{n=0}^{N} \sum_{m=0}^{M} A_{nm} x^n y^m, \tag{5}$$

where the vertex curvature radius in x direction is $r_x = 1/c_x = -452.62713$ mm and the aspherical coefficient in the x direction is $k_x = 0$; the vertex curvature radius and aspherical coefficient in the y direction are $r_y = 1/c_y = -443.4353$ mm and $k_y = 0$, respectively. The coefficients of the XY term are given in Table 2.

Without fitting for an obviously large slope variation, the basis number of the RBF model needed for fitting a double-curved freeform surface is much less compared with the basis number for fitting a bumpy paraboloid and it is set to 64. The fitting problems are also solved by least

Table 2 Coefficients of XY term.

	m					
n	0	2	4	6	8	10
0	0	6.0870E-5	1.3454E-10	3.3103E-16	1.0205E-21	1.6538E-28
1	0	−9.6572E-8	−4.4243E-13	−1.7494E-18	−6.7397E-24	—
2	8.4467E-5	3.8820E-10	1.6722E-15	7.5153E-21	−3.8004E-27	—
3	−1.7731E-8	−5.3407E-13	−4.2865E-18	−2.3053E-23	—	—
4	2.1033E-10	1.9627E-15	1.6133E-20	1.9393E-26	—	—
5	−4.4504E-14	−3.9729E-18	−4.5485E-23	—	—	—
6	1.2048E-15	2.2764E-20	9.9380E-26	—	—	—
7	−3.7513E-18	−6.5159E-23	—	—	—	—
8	1.2433E-20	1.2596E-25	—	—	—	—
9	−1.6717E-23	—	—	—	—	—
10	2.7401E-26	—	—	—	—	—

squares, with average shape factors varying from 0.2 to 0.8. The logarithm of RMS for average shape factors ranging from 0.2 to 0.8 is shown in Fig. 8. Over the shape factor range, the RMS of the RBF-SSD model is obviously lower than that of the RBF-slope model, which demonstrates a higher fitting precision.

The optimal average shape factor of the RBF-SSD model, which yielded the best fitting performances, was 0.43. For this average shape factor, the shape factors of every basis and the basis distribution are shown in Figs. 9(a) and 9(b). For the double-curved freeform surface, the slope of the edge is much larger than the slope of the center; therefore, most basis of RBF-SSD was distributed on the edge of the surface and a few were distributed on the center. Figures 9(c)

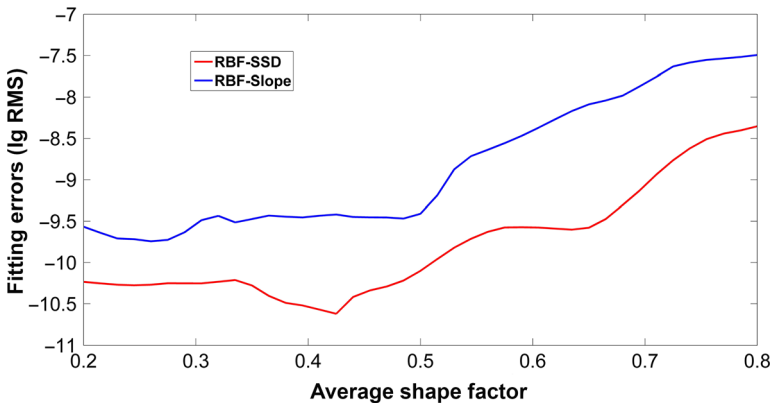

Fig. 8 Fitting performances of RBF-Slope and RBF-SSD models.

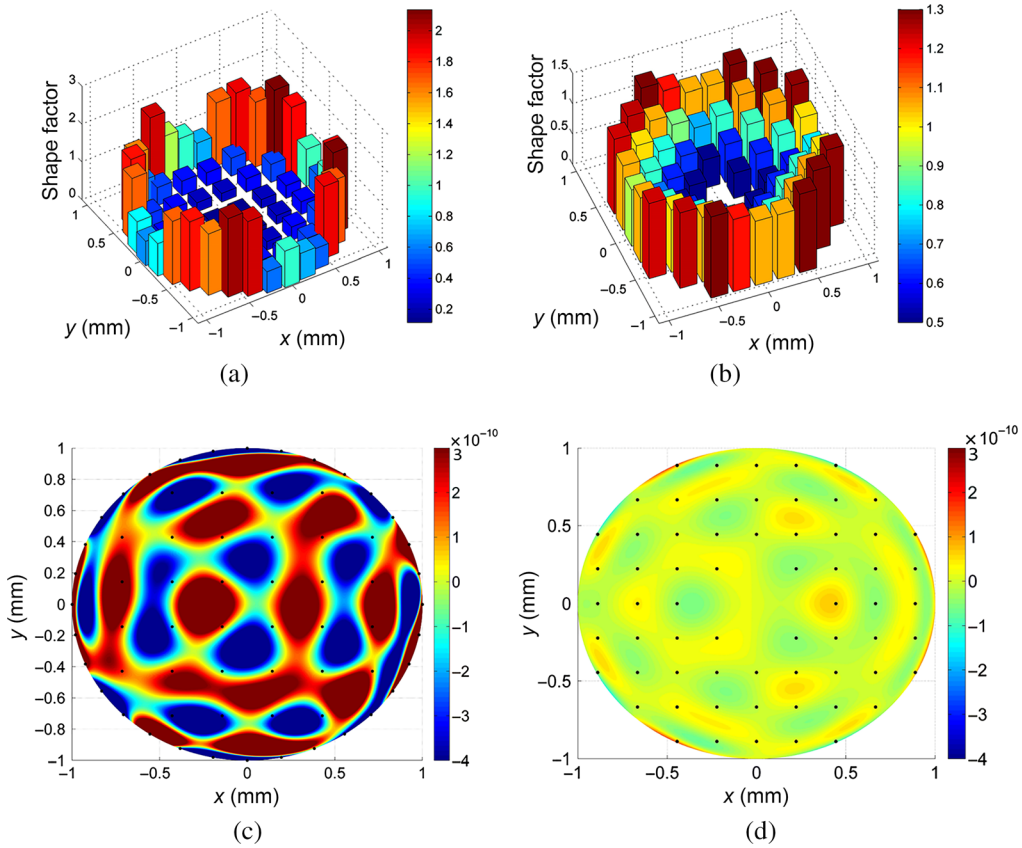

Fig. 9 Shape factors of (a) RBF-slope model and (b) RBF-SSD model. Fitting errors for (c) RBF-slope model and (d) RBF-SSD model.

and 9(d) show the basis distribution and the fitting errors over the entire aperture for the RBF-slope model and RBF-SSD model, respectively.

We can see that the RBF-SSD model showed much lower fitting RMS over the whole aperture than the RBF-Slope model, demonstrating a higher fitting precision for the double-curved freeform surface. Unlike fitting for a bumpy paraboloid, where the RBF-SSD model mainly showed better fitting results in the bumpy area, the improvement in fitting with the RBF-SSD model existed over the whole aperture in this test because double-curved freeform surfaces do not have obvious local slope variations, meantime, it can be inferred that RBF-SSD also has high fitting accuracy for nearly flat surfaces with small slope changes. With stronger fitting ability, the RBF-SSD model is superior at characterizing and is more efficient in eliminating aberrations when characterizing asymmetric surfaces in optical system designs than earlier models.

5 Design of an Off-Axis Three-Mirror System

With a stronger fitting ability, the RBF-SSD model has greater potential to obtain better performance in optical design because it is able to characterize more flexible and freeform optical surfaces. We applied the RBF-slope model and RBF-SSD model in the design of an off-axis three-mirror system. In terms of usage, this system is a reflection system applied to visible light

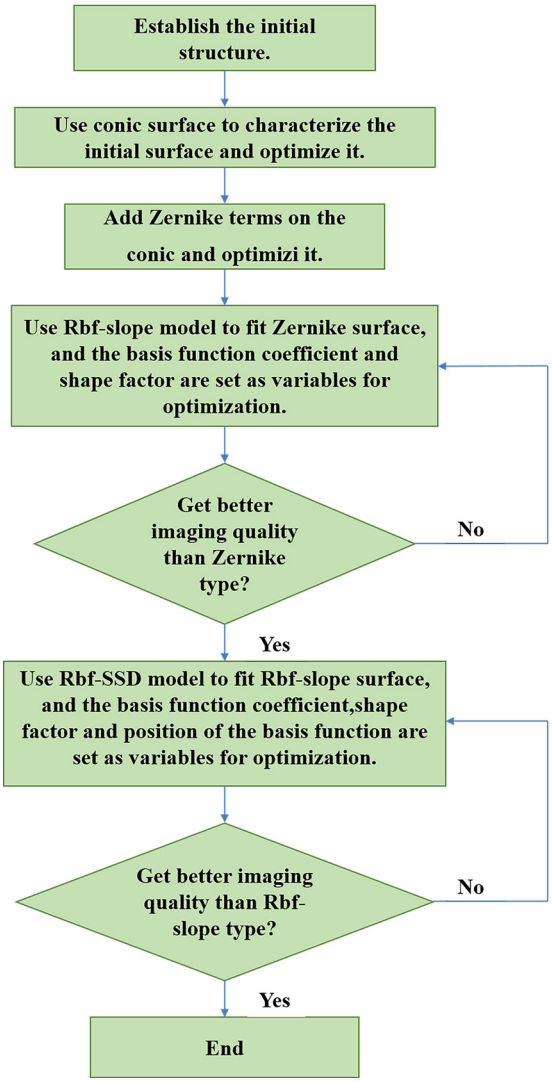

Fig. 10 Design process of RBF-SSD freeform surface.

and infrared waves. Since the reflection system has no chromatic aberration, we use 632.8nm monochromatic light as a design example. The focal length of system was 100 mm and the field of view (FOV) was $3° \times 3.6°$. In our design, the first and the second mirrors were represented by aspherical surfaces, and the third mirror was characterized by the RBF-slope model or RBF-SSD model. To compare the fitting ability between models clearly, we selected 64 RBF basis functions that are almost the maximum number of Zernike polynomial terms that CodeV can support. The design process can be illustrated by following steps.

First, the third surface of system was represented by a Zernike polynomial to build an initial structure. After optimization, the Zernike polynomial term of the third surface was fitted by the RBF-Slope model and then replaced by it. Next, the set of coefficients of each basis and shape factor variables was optimized. After obtaining a better result, the RBF-slope term of the surface was fitted by the RBF-SSD model. The overall system design process is shown in Fig. 10.

Figure 11(a) showed the sag of the RBF-slope term of the third surface, which was the target to be fitted. It can be clearly seen that the surface slope of two sides of x direction was larger than the slope of the center. To fit this surface, the shape factors of the RBF-SSD model would be larger and the basis number would be denser on two sides of the X direction, as shown in Figs. 11(b) and 11(c). Then the RBF-Slope model was replaced with the RBF-SSD model in the design and the coefficients of every basis was set as variables prior to optimization.

After optimization, the final 2D layout of the system and the sag of RBF-slope term of the third surface was shown in Fig. 12, where the third mirror was represented by the RBF-SSD model. The optical performances of the three models (Zernike polynomial, RBF-Slope, and RBF-SSD) are given in Table 3, containing the RMS wavefront error (WFE), modulation transfer function (MTF), and max distortion.

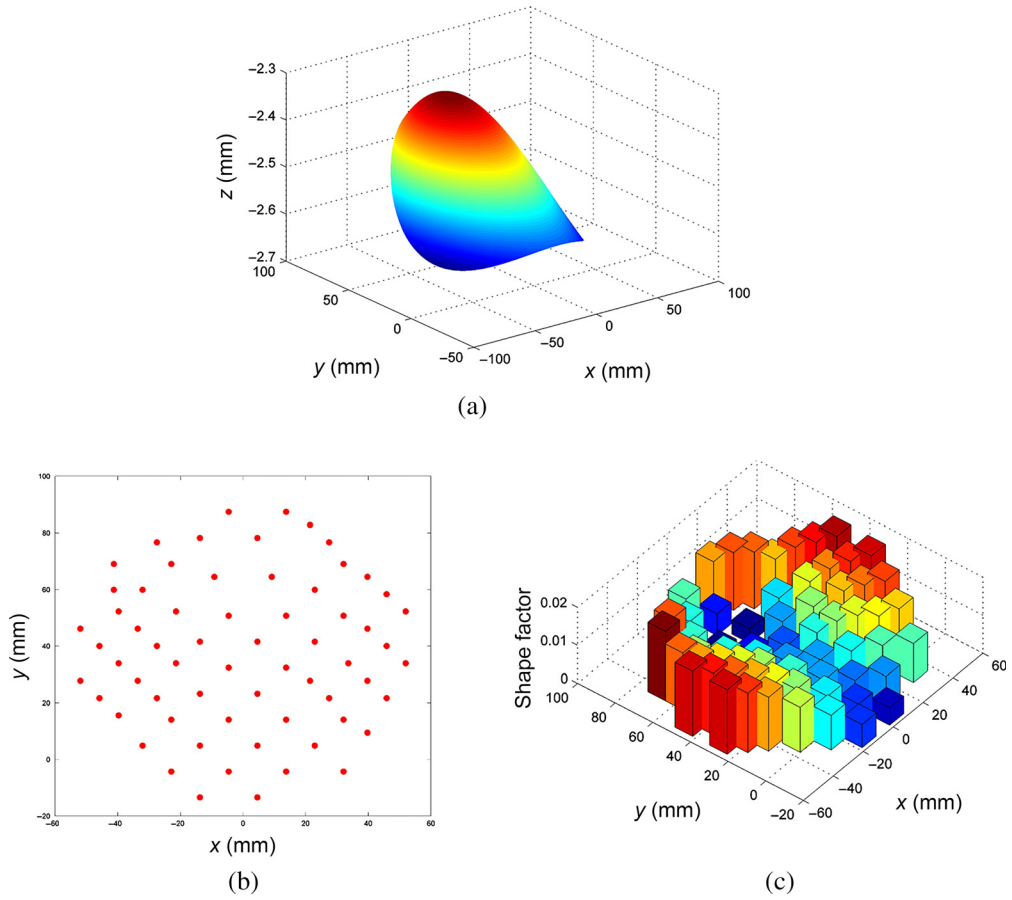

Fig. 11 (a) Sag of RBF-Slope term of the third surface. (b) Distribution of basis and (c) shape factors of RBF-SSD model for fitting the RBF-slope term of the third surface.

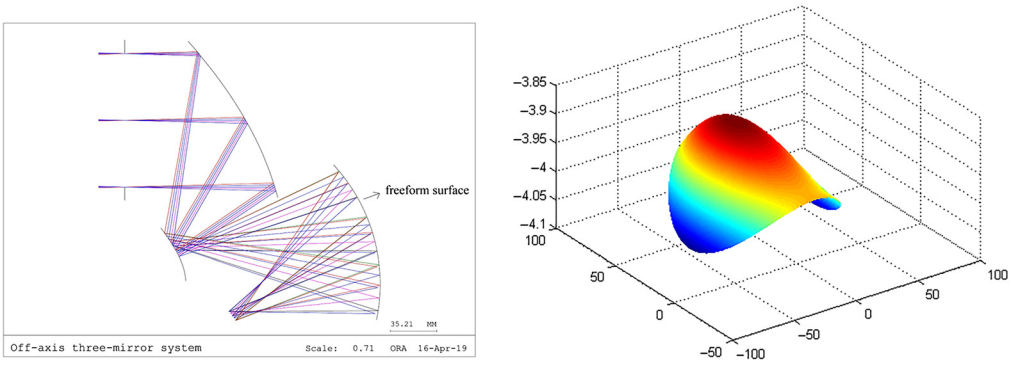

(a) (b)

Fig. 12 (a) 2D layout of the designed off-axis three-mirror system. (b) Sag of RBF-slope term of the third surface.

Table 3 Comparison of optical performance of the three models.

Model	Diffraction sine wave MTF (100 cycles/mm)	Max Distortion	RMS WFE (λ)
Zernike	0.47296	3.24	0.31144
RBF-slope	0.53855	3.15	0.28069
RBF-SSD	0.60649	3.08	0.25869

The MTF at 100 cycles/mm and RMS WFE in the full FOV for the three models were plotted in Figs. 13 and 14, respectively. Compared with the other two models, the MTF on two sides of the *X* FOV is obviously larger when applying the RBF-SSD model, meanwhile the RMS WFE also decreased for the same FOV. Owing to the relationship between the basis distribution and surface slope, the basis distributed on two sides of the *X* direction is denser than other areas to match the larger shape factors, leading to stronger fitting ability of the RBF-SSD model. With its stronger fitting ability, the RBF-SSD model has greater potential to efficiently balance aberrations in optical design and obtain great image results, which can be demonstrated by the optical performance in Figs. 13 and 14. Therefore, with the relationship between basis distribution and shape factor, the proposed RBF-SSD model can achieve a better optical performance in the design of this off-axis three-mirror system.

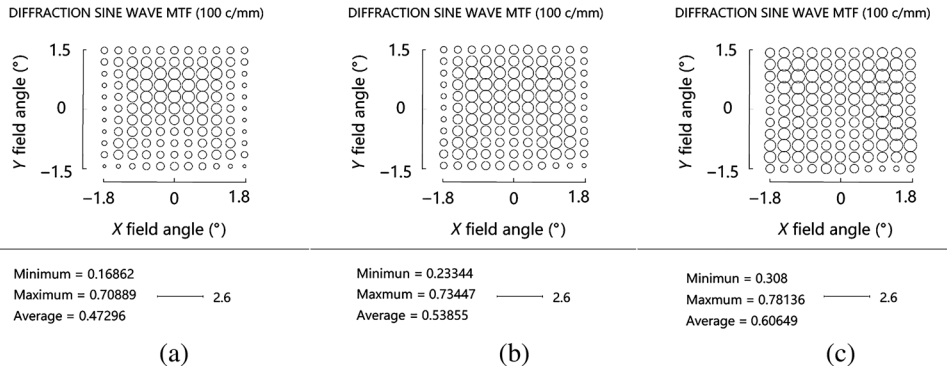

(a) (b) (c)

Fig. 13 MTF in the full FOV of the optical system with application of (a) Zernike; (b) RBF-Slope; (c) RBF-SSD models.

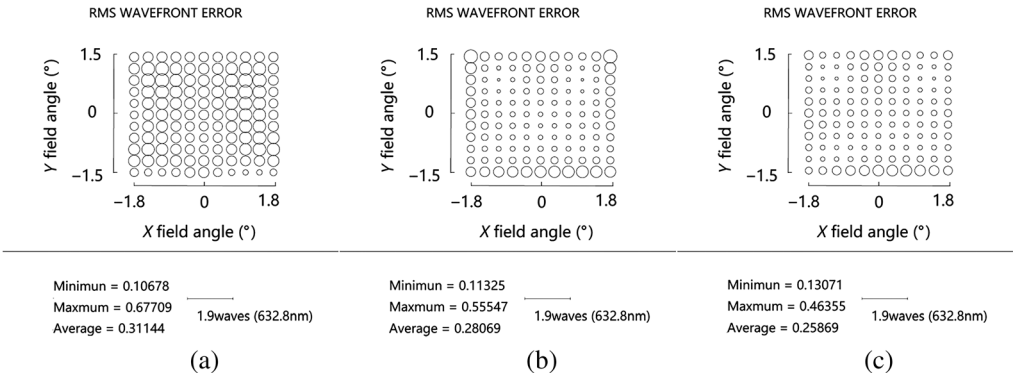

Fig. 14 RMS WFE in the full FOV of the optical system upon applying (a) Zernike; (b) RBF-slope; (c) RBF-SSD models.

6 Conclusion

We proposed a new RBF model called the RBF-SSD model for characterizing optical freeform surfaces in this paper. Relating the shape factor and basis distribution to surface slope, the RBF-SSD model had better fitting ability than the RBF-slope model. Fitting for a bumpy paraboloid and a double-curved freeform surface demonstrated the improved fitting performance of the RBF-SSD model compared to the RBF-Slope model. In the design of an off-axis three-mirror system, owing to the relationship between basis distribution and surface slope, the RBF-SSD model also showed an improved image quality compared to the other two freeform surface models. All the results showed that the RBF-SSD model can be applied in characterizing surfaces with local features in asymmetric optical systems and has potential in obtaining better image quality, replacing the classical RBF models. We will attempt to use this model in the design of other systems in the future.

Acknowledgments

This work was supported by grants from the National Key R&D Program of China (2018YFB0504400), National Natural Science Foundation of China (Grant No. 61675100), Tianjin Natural Science Foundation (Grant No. 19JCZDJC36600), and the Tianjin Key R&D Program (Grant No. 19YFZCSY00250). The authors would like to thank Changchun Institute of Optics and Mechanics, Chinese Academy of Sciences, for supporting the use of CodeV software for design simulation. The authors declare no conflicts of interest.

References

1. C. Shengqian, et al., "Design beam shapers with double freeform surfaces to form a desired wavefront with prescribed illumination pattern by solving a Monge–Ampère type equation," *J. Opt.* **18**, 125602 (2016).
2. E. Muslimov et al., "Combining freeform optics and curved detectors for wide field imaging: a polynomial approach over squared aperture," *Opt. Express* **25**, 14598 (2017).
3. S. Sorgato et al., "Compact illumination optic with three freeform surfaces for improved beam control," *Opt. Express* **25**, 29627–29641 (2017).
4. L. Wei et al., "Design and fabrication of a compact off-axis see-through head-mounted display using a freeform surface," *Opt. Express* **26**, 8550–8565 (2018).
5. R. Wu et al., "Formulating the design of two freeform lens surfaces for point-like light sources," *Opt. Lett.* **43**, 1619–1622 (2018).
6. V. F. Zernike, "Beugungstheorie des schneidenver-fahrens und seiner verbesserten form, der phasenkontrastmethode," *Physica* **1**, 689–704 (1934).
7. R. J. Noll, "Zernike polynomials and atmospheric turbulence," *J. Opt. Soc. Am.* **66**, 207–211 (1976).

8. K. Fuerschbach, J. P. Rolland, and K. P. Thompson, "A new family of optical systems employing φ-polynomial surfaces," *Opt. Express* **19**, 21919–21928 (2011).
9. G. W. Forbes, "Shape specification for axially symmetric optical surfaces," *Opt. Express* **15**, 5218–5226 (2007).
10. G. W. Forbes, "Characterizing the shape of freeform optics," *Opt. Express* **20**, 2483–2499 (2012).
11. I. Kaya, K. P. Thompson, and J. P. Rolland, "Comparative assessment of freeform polynomials as optical surface descriptions," *Opt. Express* **20**, 22683–22691 (2012).
12. I. Kaya, K. P. Thompson, and J. P. Rolland, "Edge clustered fitting grids for φ-polynomial characterization of freeform optical surfaces," *Opt. Express* **19**, 26962–26974 (2011).
13. O. Cakmakci et al., "Application of radial basis functions to shape description in a dual-element off-axis magnifier," *Opt. Lett.* **33**, 1237–1239 (2008).
14. O. Cakmakci et al., "Optimal local shape description for rotationally non-symmetric optical surface design and analysis," *Opt. Express* **16**, 1583 (2008).
15. O. Cakmakci et al., "Application of radial basis functions to represent optical free-form surfaces," in *Proc. Int. Opt. Design Conf.* pp. 424–448 (2010).
16. H. Li et al., "Design of an off-axis helmet-mounted display with freeform surface described by radial basis functions," *Opt. Commun.* **309**, 121–126 (2013).
17. Y. Wang et al., "Freeform-objective Chernin multipass cell: application of a freeform surface on assembly simplification," *Appl. Opt.* **56**, 8541–8546 (2017).
18. M. Maksimovic, "Optical design and tolerancing of freeform surfaces using anisotropic radial basis functions," *Opt. Eng.* **55**, 071203 (2016).
19. K. Tong et al., "Model of radial basis functions based on surface slope for optical freeform surfaces," *Opt. Express* **26**, 14010–14023 (2002).
20. L. Xiao et al., "A single mirror magnifier with freeform surfaces using radial basis functions based on surface slope," *Proc. SPIE* **11383**, 113830B (2020).
21. X. Lin et al., "A new orbit fitting algorithm of space-borne SAR based on householder transformation," in *Proc. Synth. Aperture Radar*, pp. 832–835 (2009).

Liuchang Xiao has achieved his master's degree in optical engineering at Nankai University. His research interests are freeform optics and optical design.

Biographies of the other authors are not available.